Journal of Material Cycles and Waste Management (2021) 23:222–230
https://doi.org/10.1007/s10163-020-01119-x

ORIGINAL ARTICLE

Recovery of iron oxide and calcium chloride from an iron-rich chloride waste using calcium carbonate

Hee Jung Yang[1] · Seok Won Yoon[1] · You Jin Kim[1] · Hee Sun Park[1] · Seok Huh[1] · Nam Hwi Hur[1]

Received: 10 March 2020 / Accepted: 14 September 2020 / Published online: 26 September 2020

Abstract

The ilmenite-chloride process has used for the production of $TiCl_4$ from the ilmenite ($FeTiO_3$) ore, which produces cyclone dust containing mostly iron chloride and includes a range of metal chlorides. The utilization of iron values present in waste chlorides of cyclone dust is becoming a crucial issue to make this process competitive. The current work demonstrates a beneficial process that can selectively separate iron values from the chloride residue. Using $CaCO_3$ as a precipitating agent, the iron component was selectively isolated from the aqueous solution of the chloride residues. The selective extraction of iron was carried out at a wide range of concentrations, and the yield of iron species was over 95%. The precipitate is in the form of $Fe(OH)_3$, which converts to Fe_2O_3 when annealed in air. In the next step, the remaining metal impurities were removed as solid precipitates through the pH tuning with CaO. Finally, $CaCl_2$ and $CaCO_3$ were obtained by adding CO_2 to the residual solution. This study provides a method of treating cyclone residues to recover $CaCl_2$ as well as $Fe(OH)_3$, which represents significant progress towards the utilization of iron-rich wastes.

Keywords Iron extraction · Chloride waste · Precipitation · Calcium carbonate · Ilmenite

Introduction

Ilmenite is an abundant titanium-bearing mineral. In ilmenite with the idealized formula of $FeTiO_3$, iron (Fe) and titanium (Ti) metals form alternating bi-layers perpendicular to the *c* direction and octahedrally coordinate to oxygen ions [1]. It was used as a starting raw material to produce titanium tetrachloride ($TiCl_4$) by the chloride process [2, 3]. Ilmenite is much cheaper than rutile, which might be advantageous for making the process economical. Another advantage is that ilmenite has a layered structure, which can readily break down into iron and titanium chlorides, respectively [4]. Due to the presence of large amounts of iron impurities in ilmenite, however, high-grade rutile composed of over 95% TiO_2 typically uses as a feedstock for the commercial chloride process.

In the ilmenite-chloride process [5], ilmenite converts to a mixture of metal chlorides in a chloride stream, which can broadly divide into volatile and non-volatile chlorides [6]. Titanium tetrachloride with a boiling point of 136 °C is the primary volatile chloride collected as a liquid product through the condensation process [7]. Non-volatile chlorides are solid residues accumulated in the chlorinator, which are separated by a cyclone. The solid chloride residues mostly contain iron chloride together with small amounts of other metal chlorides, which are corrosive and hazardous. Solid wastes cannot be disposed of at a general waste disposal site because they cause environmental problems [8]. Accordingly, they will have a detrimental impact on the entire process if they are not recycled. For this ilmenite-chloride process to be environmentally benign and economically viable, it requires not only the selective separation of metal values from the chloride residues but also is necessary to utilize them as value-added products. Mainly, separating and recycling iron species are essential for the efficient use of the ilmenite ore because about 42–57 wt% of iron oxides are typically present in the ore [9]. For instance, iron oxides prepared in this way can be used as high-quality

Electronic supplementary material The online version of this article (https://doi.org/10.1007/s10163-020-01119-x) contains supplementary material, which is available to authorized users.

✉ Nam Hwi Hur
nhhur@sogang.ac.kr

[1] Department of Chemistry, Sogang University, Seoul 04107, Republic of Korea

pigments to create distinctive colors in cosmetics, paints, and other decorative applications.

The solvent extraction method is employed to recover iron values from various iron-containing wastes such as cyclone dust from the chloride process [10–13], spent acids [14–18], and metallurgical wastes [19, 20]. A wide range of extracting solvents including methyl isobutyl ketone [21, 22], tri-*n*-butyl phosphate [23], phosphoric acid derivatives [24, 25], various phosphine oxides [26, 27], and ionic liquids [28–32] have been investigated, which are effective to selectively extract iron species. However, this method requires a multi-step process, including separation, purification, and concentration [33]. Even worse is that this process requires lots of harmful organic solvents and expensive reagents. Thus, it is thus of great importance to developing new separation methods that use in the absence of organic solvents and expensive reagents, which will reduce environmental impacts as well as operating costs.

Precipitation techniques are also well-known methods for recovering valuable metals from mixed metal solutions only by the addition of precipitating agents [34–40]. However, this method makes it difficult to selectively separate a specific metal from the mixed solution due to a small difference in their solubility products. Another drawback is that conventional techniques known thus far cannot separate coprecipitated metal impurities. Herein, we report a two-step process for separating iron values selectively from chloride wastes generated in the ilmenite-chloride process. This process is developed based on the precipitation reaction between basic $CaCO_3$ powder and acidic chloride solution. The chloride stock solution was prepared according to the composition of the ilmenite ore and residual waste, which could simulate the behavior of cyclone dust produced in the ilmenite-chloride process. By adding $CaCO_3$, iron species were selectively isolated as solid sediments in the form of $Fe(OH)_3$.

Moreover, $CaCl_2$ was obtained by the addition of CO_2 to the remaining solution that contains large quantities of chloride ions. Therefore, this process using abundant $CaCO_3$ as a precipitating agent is an economically viable and environmentally benign method because it can simultaneously produce useful products like $CaCl_2$ and $Fe(OH)_3$ from the waste chloride residues. For the synthesis of iron oxide from chloride residues, it is common to use an alkaline precipitant like NaOH. Surprisingly, we found that $CaCO_3$ can also use as a finely ground powder-type sedimentation reagent.

Experimental

Materials

All the chemicals were obtained from commercial suppliers and were used without further purification. Ferric chloride ($FeCl_3$, 97%), manganese chloride ($MnCl_2$, 99+%), chromium chloride ($CrCl_2$, 95%), and calcium oxide (CaO, 99.995%) were purchased from Sigma Aldrich (St. Louis, USA). Magnesium chloride ($MgCl_2$, 99.9%) and calcium carbonate ($CaCO_3$, 99.99%) were purchased from Kojundo Chemical Laboratory (Saitama, Japan). Anhydrous aluminum chloride ($AlCl_3$, 99.9%) was purchased from Tokyo Chemical Industry (Tokyo, Japan).

Preparation of a stock solution

The present investigation on the extraction of valuable species used analytical data for the ilmenite ore sample kindly given by the Research Institute of Industrial Science and Technology at Pohang, Korea. An inductively coupled plasma-atomic emission spectroscopy (ICP-AES) was employed to determine elemental compositions of the ilmenite. The standard solution for the extraction study was made based on the determined compositions. The ICP-AES data in Table 1 show all elements present in the ore, which include Ti, Fe, Si, Mn, Al, Mg, Cr, Ca, and V. In the ilmenite-chloride process, titanium (Ti) chloride and vanadium (V) chloride are simultaneously separated as volatile components at the end of the chlorinator due to the proximity of their boiling points. The non-volatile chlorination products, which are collected in the chlorinator by a cyclone, could be $FeCl_3$, $MnCl_2$, $AlCl_3$, $MgCl_2$, $CrCl_2$, and $CaCl_2$. Silica (SiO_2) is not easily chlorinated and remains unreacted. Small traces of calcium species were ignored because they can be separated as calcium chloride ($CaCl_2$) at the end of the present process. For this reason, we prepared an aqueous solution containing Fe, Mn, Al, Mg, Cr ions, which used as a stock solution for extraction study. A three-neck round bottom flask with a magnetic stirring bar was charged with five metal chlorides in an argon-filled glove box, which include $FeCl_3$ (18.192 g, 112.0 mmol), $MnCl_2$ (0.680 g, 5.4 mmol), $AlCl_3$ (0.512 g, 5.2 mmol), $MgCl_2$ (0.340 g, 3.6 mmol), and $CrCl_2$ (0.284 g, 2.3 mmol). After moving the flask into a fume hood, 100 mL of deionized water was added to the flask. The mixture was stirred at room temperature for 30 min, which led to a completely dissolved solution. The resulting solution was used as a stock solution for the extraction study.

Table 1 Typical metal compositions (wt%) of ilmenite ore analyzed by an ICP-AES

Element	Ti	Fe	Si	Mn	Al	Mg	Cr	Ca	V
wt%	32.15	26.99	1.15	0.99	0.77	0.50	0.42	0.20	0.12

Precipitation of iron species

Precipitation experiments were carried out in a round bottom flask at room temperature. The amount of $CaCO_3$ added to the 10 mL stock solution was increased at 2.0 mmol intervals, and the pH change was carefully monitored. The brown sediment was formed with the addition of $CaCO_3$ over 14.0 mmol. Accordingly, 14.8, 15.0, and 15.2 mmol of $CaCO_3$ were divided into individual sets and precipitation experiments were conducted. Typically, 14.8 mmol of $CaCO_3$ was added to 10 mL of the stock solution, and the mixed solution was stirred for 6 h. The brown precipitate slowly formed and was separated from the solution by centrifugation. The separated solution was stored for the next experiment. The resulting precipitate was washed with water several times and then dried in an oven at 80 °C for 10 h. The dried powder (FeOOH) was converted into iron oxide (Fe_2O_3) by calcination at 600 °C for 6 h in air. The same experiment was repeated by adjusting the amount of $CaCO_3$ to 15.0 and 15.2 mmol. And the correlation between the $CaCO_3$ amount and the yield was examined along with the pH change.

Removal of residual metal species and recovery of calcium chloride

To remove residual metal species as solids, CaO was added to the separated solution until the pH is above 12. The solution was then stirred for 3 h at room temperature. Dark brown precipitates were formed, which were collected from the solution by centrifugation. The precipitates were washed with water several times and then dried in an oven at 80 °C for 10 h. The dried powder was annealed at 800 °C for 5 h in the air to make the powder crystalline, which enables to confirm that all the remaining metal components were removed from the solution. The separated solution is basic and contains a large amount of calcium and chloride ions. The CO_2 gas was bubbled into the solution for 3 h, which led to the formation of white precipitates. The precipitated solid was separated from the solution by centrifugation. The precipitates were washed with water several times and then dried in an oven at 80 °C for 10 h, which were found to be $CaCO_3$. About 0.05 g of $CaCO_3$ was obtained. Polycrystalline $CaCl_2$ was grown from a residual solution by slowly evaporating water. The amount of $CaCl_2$ obtained was 2.76 g, and the yield was 98.6% according to the amount of $CaCO_3$ added.

Characterization

Elemental compositions of the ilmenite ore sample and extracted products were determined using an ICP-AES. Powder X-ray diffraction (XRD) measurements were performed on a Rigaku DMAX 2500 diffractometer (Rigaku, Japan) with Cu Kα radiation ($\lambda = 1.5406$ Å) operated at 40 kV and 15 mA. Thermogravimetric analysis was carried out using a TGA 2050 instrument (TA Instruments, USA). The sample was placed on a platinum pan for each run and analyzed in air or oxygen from 25 to 800 °C at a heating rate of 5 °C/min. A Thermo Orion Star A211 pH meter with an electrode stand was used for recording pH in the mixed chloride solution. High-resolution transmission electron microscopy (HRTEM) was performed on a JEOL JEM-2100 F microscope (JEOL, Japan). High-resolution scanning electron microscopy analyses were carried out using a Hitachi S-5500 microscope (Hitachi, Japan).

Results and discussion

Precipitation of iron species from a mixed metal chloride solution

For the precipitation study, we made a stock solution based on metal compositions in an ilmenite sample. The mixed chloride solution was prepared by dissolving stoichiometric amounts of $FeCl_3$, $MnCl_2$, $AlCl_3$, $MgCl_2$, and $CrCl_2$ in water. Their concentrations are ranged from 0.023 to 1.124 M, depending on their weight percentage. Detailed data regarding the stock solution are given in Table 2. Using this solution, we derived the precipitating agents and process parameters necessary for the selective precipitation of iron species and $CaCl_2$.

The selection of an appropriate precipitating agent is vital for the effective separation of iron species in the mixed

Table 2 Weight percentages and molar concentrations of metal chlorides in the stock solution based on the ICP-AES data of ilmenite ore

	$FeCl_3$	$MnCl_2$	$AlCl_3$	$MgCl_2$	$CrCl_2$
g in 100 mL DDW	18.192	0.680	0.512	0.340	0.284
Concentration [M]	1.124	0.054	0.052	0.036	0.023
K_{sp}[a]	6.3×10^{-38}	2.0×10^{-13}	1.0×10^{-32}	5.6×10^{-12}	1.0×10^{-17}
Expected pH	1.58	8.28	3.76	9.10	6.32

The solubility product constant (K_{sp}) value is that of the corresponding metal hydroxide. The expected pH value corresponds to the concentration at which metal ions precipitate in the form of metal hydroxides

[a]K_{sp} is the equilibrium constant for the following reaction: $M(OH)_x \leftrightarrow M^{x+} + x\ OH^-$

chloride solution. The chloride solution has a strong acidity, and the pH is typically less than 1.0 [41]. It is thus natural to evaluate a basic reagent such as NaOH for precipitating agent. However, the addition of aqueous NaOH solution into the chloride solution often leads to the coprecipitation of iron and other metal species. We found that selective precipitation of iron components using NaOH is possible only in very narrow concentration ranges. It is thus difficult to implement this method in the actual process. Instead of a strong base like NaOH, we therefore used weak basic calcium carbonate ($CaCO_3$) as a precipitant. We surprisingly found that only iron species could be selectively separated in a flexible manner. Calcium carbonate is an economical and very efficient reagent because it is cheap and can be added directly to the solution in the form of a powder. Therefore, precipitation studies were carried out using $CaCO_3$ as a precipitating agent.

The addition of $CaCO_3$ to the chloride solution raises the pH, resulting in the formation of hydroxide precipitates. One of the crucial factors in determining whether the precipitates form is the solubility product constant (K_{sp}). The K_{sp} value indicates the degree to which a solid compound dissolves in an aqueous solution. The pH value at which metal ions precipitate in the form of metal hydroxides can be calculated from the K_{sp} data and the concentration of metal ions. The calculated pH values and the K_{sp} data of representative metal hydroxides are listed in Table 2. The K_{sp} value of $Fe(OH)_3$ is 6.3×10^{-38}, which is the lowest value compared to those of other metal hydroxides. The lowest K_{sp} value means that iron ions precipitate into $Fe(OH)_3$ before other metal ions. When Fe^{3+} ions precipitate, the expected pH of the solution is 1.58. This value is also lower than those of other metal hydroxides. It is thus possible to selectively separate iron components through the pH adjustment. It is worth mentioning that the pH value calculated for $Al(OH)_3$ is 3.76 and does not differ significantly from that of $Fe(OH)_3$. Therefore, the use of $CaCO_3$ as precipitant could be more effective at selectively separating iron species from the chloride solution than the strong base NaOH.

Figure 1 illustrates the pH change of the mixed chloride solution according to the amount of $CaCO_3$ added. $CaCO_3$ is sparingly soluble in water (47 mg/L at 25 °C). In acidic media, however, it quickly disintegrates into Ca^{2+}, CO_2, and H_2O as follows: $CaCO_3 + 2H^+ \rightarrow Ca^{2+} + CO_2 + H_2O$. During the precipitation process, $CaCO_3$ is completely dissolved. The pH change was measured after the complete dissolution of added $CaCO_3$. When $CaCO_3$ is added to the chloride solution with an initial pH of about 0.70, the pH slowly increases to about 1.48. The pH of the solution hardly increases until 13.0 mmol of $CaCO_3$ is added and then rapidly increases from 14.0 mmol of $CaCO_3$ added. There is a buffer region between 2.0 and 13.0 mmol in the amount of $CaCO_3$ added. In this region, Fe^{3+} ions gradually change

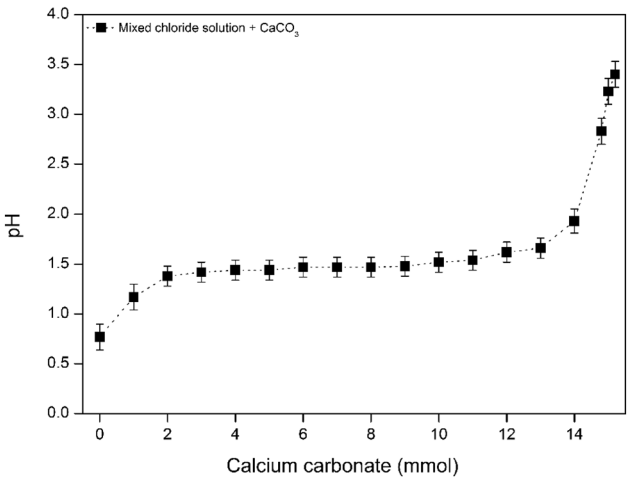

Fig. 1 The pH changes of the mixed chloride solution as a function of $CaCO_3$ added. The amount of $CaCO_3$ added denotes as mmol

to $Fe(OH)_3$, and Ca^{2+} ions react with Cl^- ions to convert to $CaCl_2$. As a result, the pH does not rise even if $CaCO_3$ adds to this buffered state. The iron hydroxide formed dissolves initially at low pH but begins to precipitate as the pH approaches 2.0. This experimental result is consistent with the calculation value that precipitation starts around pH 1.58 (See Table 2). It is worth mentioning that the pH change curve is analogous to the titration curve for a strong acid with a weak base.

Through the drying process, the initial precipitate, $Fe(OH)_3$, turns into a brown powder. Powder XRD analysis, given in the top panel of Fig. 2, shows that the dried brown powder is FeOOH. When the powder is further annealed at high temperature in air, it converts to highly crystalline iron oxide in red color. The bottom panel of Fig. 2 shows the XRD pattern of the annealed sample. All diffraction peaks are in good agreement with those of Fe_2O_3 with the hematite structure, showing the formation of the desired cubic phase. The absence of other peaks suggests that no other metal hydroxides appear to precipitate simultaneously. Further, the purity of Fe_2O_3 was confirmed to be 96.26% by the ICP-AES analysis. Figure S1 shows TEM and Elemental mapping images of representative Fe_2O_3 particles, illustrating that the particle has a cubic shape.

Thermal changes of the precipitate, $Fe(OH)_3$, were investigated using thermal gravimetric analysis (TGA). Figure 3 reveals that the weight percentage of the precipitate decreases to about 69.1% over the original weight upon heating, which is lower than the theoretical value (74.71%) for complete conversion of $Fe(OH)_3$ into Fe_2O_3. The low value suggests that precipitate contains solvent molecules like water. After TGA measurement, powder XRD of the specimen is virtually identical with the XRD profile of Fe_2O_3 in Fig. 2.

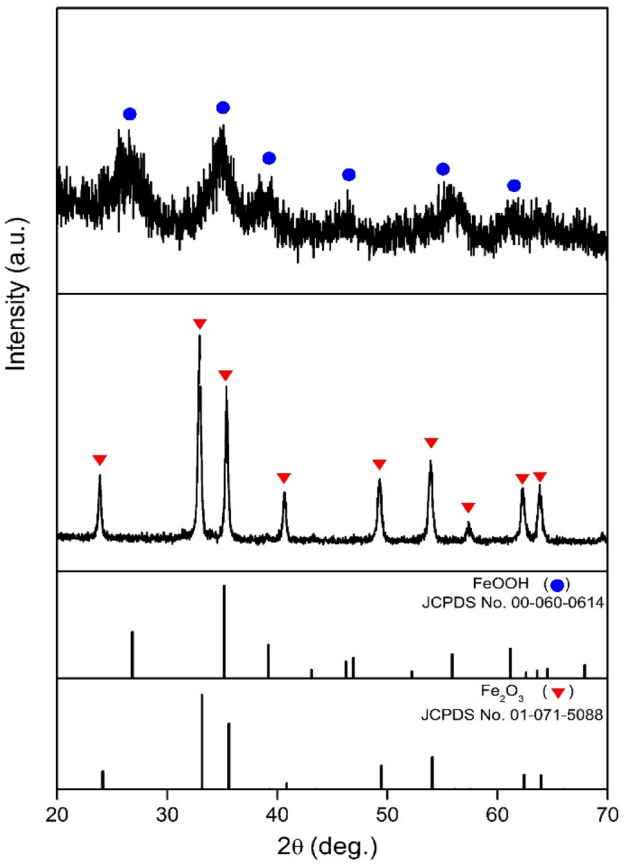

Fig. 2 Powder XRD profiles of precipitates dried at 80 °C (top panel) and annealed in air at 800 °C (bottom panel). The precipitate was obtained using 15.2 mmol of $CaCO_3$ as a precipitating agent. All the diffraction peaks of top and bottom panels can be well indexed to the FeOOH and Fe_2O_3 phases, respectively. The vertical bars below the XRD profiles indicate the calculated positions for the Bragg reflections of FeOOH (blue circles) and Fe_2O_3 (red triangles)

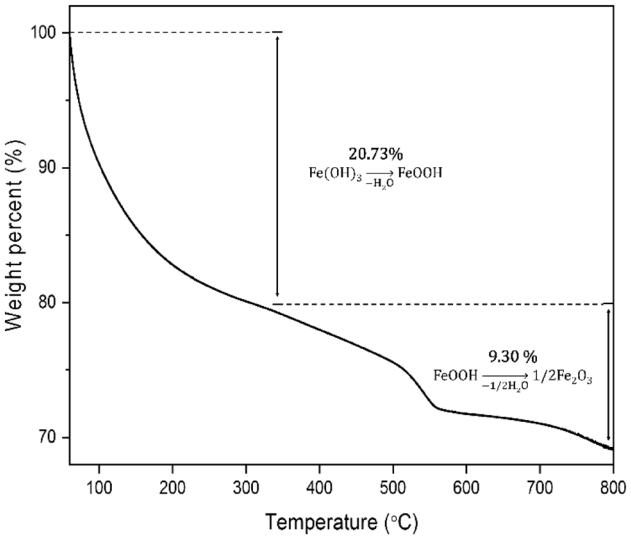

Fig. 3 Thermogravimetric analysis (TGA) data for the precipitate obtained using $CaCO_3$ as a precipitant. Data were collected in the air at a heating rate of 5 °C/min

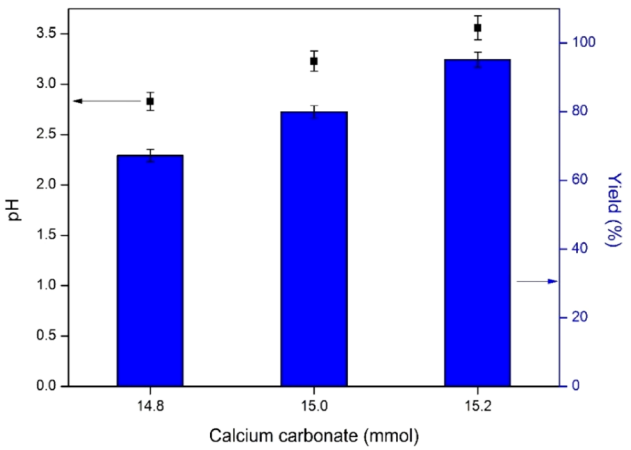

Fig. 4 The pH value on the left vertical axis was measured from the supernatant remaining after the precipitate had formed. The right vertical axis represents the yield (%) of Fe_2O_3 produced according to the amount of $CaCO_3$ added

As anticipated, the amount of hydroxide precipitates increases with increasing pH. Additional experiments performed to determine the purity and yield of the product according to the added $CaCO_3$. The precipitation occurred in the pH range above 2.0. The precipitate was separated from the supernatant by centrifugation. Figure 4 shows the change in pH and yield, depending on the amount of $CaCO_3$ added. The separated precipitate was washed several times using deionized water and then dried sufficiently in the oven, followed by calcination at 600 °C in air. The yield was determined based on the amount of iron oxide (Fe_2O_3) finally obtained by heat treatment. The pH value is a measure of the pH of the supernatant formed by the addition of $CaCO_3$. The yield increases with increasing the pH, but other metal ions can also precipitate in hydroxide form when the pH increases. Thus, the experiment was performed at a pH lower than 3.76 because $Al(OH)_3$ could precipitate around pH 3.76. When 15.2 mmol of $CaCO_3$ was added, the yield was 95.17%, and the pH of the supernatant was 3.56. The ICP-AES analysis determined the purity of Fe_2O_3 in the final product, which was about 96.26%. Detailed ICP-AES data of Fe_2O_3 is given in Table 3. The mass percentages of the two iron oxides recovered using 14.8 mmol and 15.0 mmol of $CaCO_3$ were determined to be 97.29 and 97.07%, respectively. It is worth noting that the commercial use of iron oxide is heavily dependent on the purity of iron oxide. Highly pure iron oxides composed of over 99% Fe_2O_3 are used as raw materials for cosmetics, sensors, and catalysts [42, 43]. On the other hand, iron oxides of relatively

Table 3 ICP-AES results of iron oxide (Fe_2O_3) recovered using 15.2 mmol of $CaCO_3$

Element	Fe	Mn	Al	Mg	**Cr**
Concentration (ppm)	–	1409.6	8921.9	349.5	9821.8
Mass ratio (%)	96.26	0.16	1.82	0.35	1.73

The iron oxide was obtained by annealing the precipitates at 600 °C in air

Table 4 Change in pH of the residual solution according to the amount of CaO added

	1st addition	2nd addition	3rd addition	4th addition
CaO (mmol)	0.36	0.54	0.71	0.89
pH change	4.1 → 7.4	6.6 → 9.2	8.2 → 9.4	8.4 → 11.2

The addition was divided into four additions

low purity (90%-95%) are widely used for pigments [44, 45]. Thus, iron oxides of about 96% purity synthesized by the current method are suitable for use as a pigment.

Removal of other metal species from a solution remaining after iron precipitation

The residual supernatant after the recovery of iron species is usually treated as wastewater. However, the recovery of calcium and chloride ions as $CaCl_2$ from the remaining solution can make the whole process more economical. In the second experiment, we first removed residual metal ions by precipitating them with calcium oxide (CaO). As can be seen from the calculated pH values in Table 2, all-metal ions form precipitates in the form of hydroxides when the pH of the solution increases. CaO was chosen as a precipitant because it not only has strong basicity but also contains a calcium ion. To analyze the pH change and precipitate depending on the amount of CaO added, CaO was added to the solution in four portions. Table 4 shows the pH change depending on the amount of CaO added. All the precipitates were annealed in air at 800 °C to increase their crystalline property, and then their X-ray diffraction data were collected. This calcination step is crucial for accurate structural analysis because the precipitate initially formed are less crystalline.

The second experiment was conducted with a residual solution after recovering iron species with 15.2 mmol of $CaCO_3$. When 0.36 mmol of CaO is added to the solution (1st addition, see Table 4), the pH rises to about 7.4, resulting in a brown precipitate. Calcium oxide reacts with water to form calcium hydroxide, $Ca(OH)_2$, which is soluble in the acidic chloride solution. At high pH value, however, its solubility drastically decreases, which results in the formation of $Ca(OH)_2$. XRD pattern of the first precipitate annealed in air showed that the precipitate contained $CaFe_2O_4$, $CaFeO_3$, and $Ca_2Fe_2O_5$ phases. The impurities suggest that the remaining iron ions, after the first step, dropped to precipitation along with Ca ions as the pH increased.

Adding 0.54 mmol of CaO to the residual solution raises the pH to 9.2 (2nd addition), forming a second precipitate. XRD data of the second precipitate show that the precipitate contains $Ca_3Al_2O_6$ and $CaCrO_3$. This result is in good agreement with the tendency of pH to form precipitates shown in Table 2. XRD analysis of the precipitate obtained from the third addition of CaO shows that $CaMn_2O_4$ and $CaMnO_3$ are major phases. Finally, 0.54 mmol of CaO is added to the residual solution, the pH rises to 11.2, and all remaining manganese and magnesium ions precipitate. As expected from the K_{sp} values in Table 2, it can be seen that iron ions form hydroxide precipitates at the lowest pH, and other precipitates are formed in the order of Al, Cr, Mn, and Mg as the pH increases. The pH change, according to CaO addition, is given in Table 4 and the XRD data of the precipitates at each addition are shown in Fig. 5. After metal ions are entirely removed by adding CaO, an aqueous solution exclusively composed of calcium and chlorine ions remains. The same experiments were performed with two residual solutions after the iron recovery with 14.8 mmol and 15.0 mmol of $CaCO_3$. The pH changes with the amount of $CaCO_3$ are summarized in Table S1 and S2. Corresponding XRD profiles are illustrated in Fig. S2 and S3.

Recovery of $CaCl_2$ from a solution remaining after precipitation of all-metal species

The pH of the residual supernatant after precipitation of all metal ions is about 11. This basic aqueous solution contains many Ca^{2+} and Cl^- ions. And $Ca(OH)_2$ is also present as an equilibrium product in solution, which can react with CO_2 to form $CaCO_3$ [46, 47]. Blowing CO_2 gas into the supernatant readily produces a white precipitate ($CaCO_3$). The precipitates were removed by centrifugation. The remaining solution was neutral, with a pH of about 7.2. After drying the precipitate in an oven, it was examined by XRD and found to be $CaCO_3$ (See Fig. 6a). The $CaCO_3$ powder created by the reaction of $Ca(OH)_2$ and CO_2 can be reused in the first process to separate iron species from the chloride waste. In the separated solution, polycrystalline $CaCl_2$ formed through the evaporation of water. Typically, $CaCl_2$ was obtained in the hydrate form of $CaCl_2$. Heat treatment converts hydrated $CaCl_2$ to anhydrous $CaCl_2$. Figure 6b shows the XRD pattern of hydrated $CaCl_2$ obtained by the slow evaporation of water. The XRD pattern matches well with that of $CaCl_2{\cdot}4H_2O$.

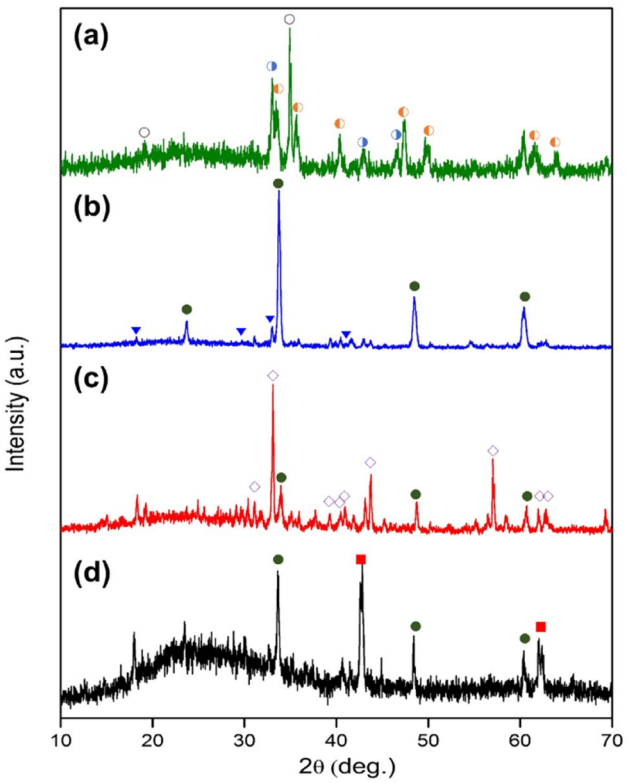

Fig. 5 Powder XRD profiles of four precipitates obtained by precipitation of the residual solution with CaO. The XRD data were collected after calcination of the precipitates in the air at 800 °C. The order of the XRD patterns from the top to the bottom panel corresponds to those of the first, second, third, and fourth precipitates, respectively: **a** first precipitates: $CaFe_2O_4$ (right side black shaded circle), $CaFeO_3$ (white dot), $Ca_2Fe_2O_5$ (left side black shaded circle); **b** second precipitates: $Ca_3Al_2O_6$ (iverted black triangle), $CaCrO_3$ (black dot); **c** third precipitates: $CaMn_2O_4$ (white diamond), $CaMnO_3$ (black dot); **d** fourth precipitates: $CaMnO_3$ (black dot), MgO (black square)

Flowsheet for the recovery of iron oxide and calcium chloride

A schematic of the precipitation process developed in this study is shown in Fig. 7. This process for the recovery of iron oxide and calcium chloride from the chloride solution consists of three significant steps. Each step was described in detail in the previous paragraphs. The first step is to separate iron species from the solution of mixed metal chlorides using $CaCO_3$ as a precipitating agent. At this stage, almost all iron ions are precipitated in hydroxide form, $Fe(OH)_3$, and other metal ions remain in solution. The second step is the removal of all metal ions in the solution by precipitation in the form of hydroxides. At this stage, CaO, which is a strong base, is used as a precipitation agent. The third step is to crystallize $CaCl_2$ in a solution in which all the metal components were removed. The solution is neutralized by blowing CO_2 into the solution, which results in the formation of $CaCO_3$. After separating the $CaCO_3$ solid, water in the remaining solution is evaporated to yield $CaCl_2$.

Conclusion

We have developed a novel method to selectively recover iron values from iron-rich chlorides using environmentally benign and abundant $CaCO_3$ powders as precipitants. This process makes it possible to selectively precipitate iron species from the chloride solution and easily produce $CaCl_2$ from residual supernatant. When $CaCO_3$ was added until the pH of the solution was over 3.3, more than 95% of the iron species with high purity was separated from the chloride solution. $CaCl_2$ can also be obtained from

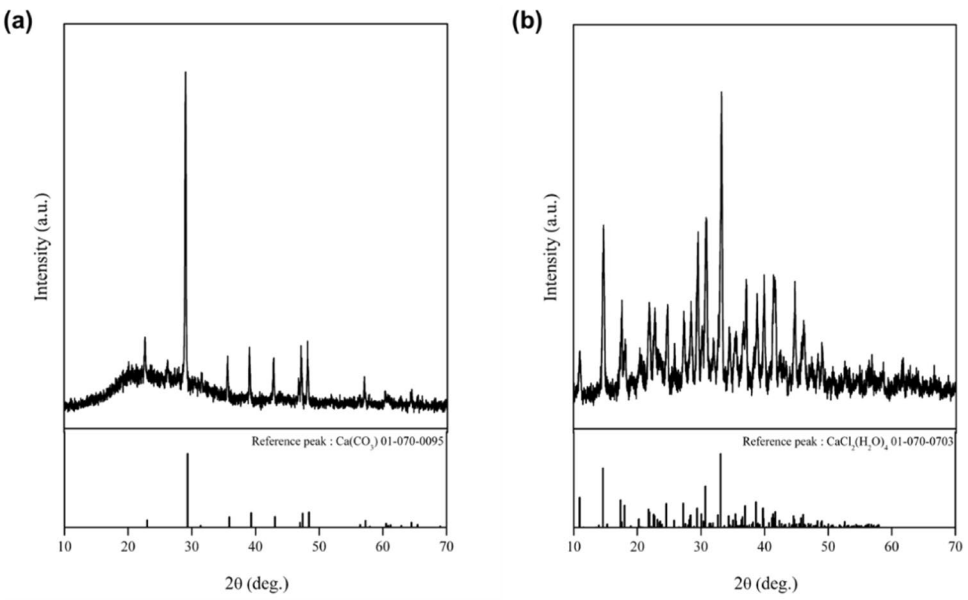

Fig. 6 **a** Powder XRD pattern of $CaCO_3$ obtained by bubbling CO_2 into the residual solution. **b** Powder XRD profile of hydrated $CaCl_2$ obtained by the evaporation of water in the separated solution. The vertical bars below the XRD profiles indicate the calculated positions for the Bragg reflections of **a** $CaCO_3$ and **b** $CaCl_2{\cdot}4H_2O$

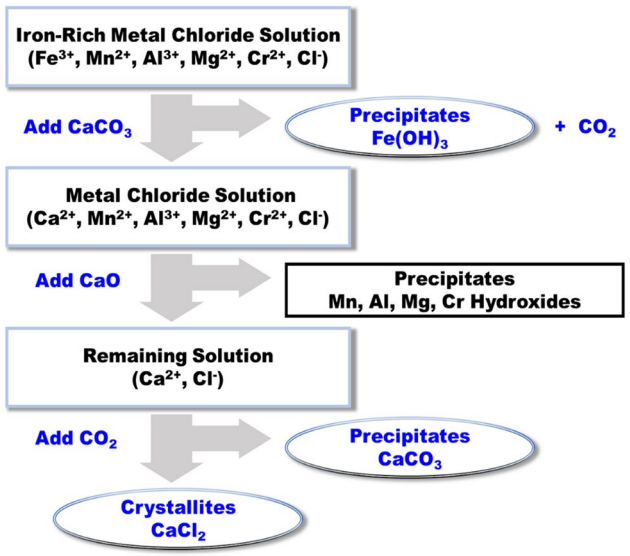

Fig. 7 Overall schematic flow diagram for the precipitation process developed in this study

the remaining solution by flowing CO_2 gases. The present work demonstrates the potential of $CaCO_3$ for environmentally friendly process design with regard to recovery of iron species from calcium chloride waste, which enables to use ilmenite extensively as a feedstock for $TiCl_4$ production.

Acknowledgements This work was supported by the Technology Innovation Program, funded by the Ministry of Trade, Industry & Energy (MOTIE, Korea) under contract number 10052751. This work was also supported by the "Human Resources Program in Energy Technology" of the Korea Institute of Energy Technology Evaluation and Planning (KETEP), granted financial resources from the MOTIE (Korea) through the grant number 20174010201150.

References

1. Sibum H, Güther V, Roidl O, Habashi F, Wolf H-U (2000) Ullmann's encyclopedia of industrial chemistry, Edition: electronic release, Chapter: titanium, titanium alloys, and titanium compounds. Wiley-VCH, Weinheim, pp 1–35
2. Wensheng Z, Zhaowu Z, Chu Y-C (2011) A literature review of titanium metallurgical processes. Hydrometallurgy 108:177–188. https://doi.org/10.1016/j.hydromet.2011.04.005
3. Mehdilo A, Irannajad M (2012) Effects of mineralogical and textural characteristics of ilmenite concentrate on synthetic rutile production. Arab J Geosci 6:3865–3876. https://doi.org/10.1007/s12517-012-0647-x
4. Yuan Z, Wang X, Xu C, Li W, Kwauk M (2006) A new process for comprehensive utilization of complex titania ore. Miner Eng 19:975–978. https://doi.org/10.1016/j.mineng.2005.10.002
5. Fu X, Wang Y, Xiong L, Wei F (2009) Enhancement of the low temperature chlorination of ilmenite with CCl_4 by adding Cl_2. J Alloys Compd 486:365–370. https://doi.org/10.1016/j.jallcom.2009.06.149
6. Perkins E-C, Lang R-S, Dolezal H (1961) Chlorination of an Idaho ilmenite. [Washington, D.C.]: U.S. Dept. of the Interior, Bureau of Mines.
7. Joseph P-T, Mathew P-M (1969) A new method of processing ilmenite for titanium compounds. J Chem Soc D. https://doi.org/10.1039/C29690000374
8. Bordbar H, Yousefi A-A, Abedini H (2017) Production of titanium tetrachloride ($TiCl_4$) from titanium ores: A review. Polyolefins J 4:149–173. https://doi.org/10.22063/poj.2017.1453
9. Raman R, Aarti K, Deepika K-S, Ranjit P, Ranganathan S (2019) Carbothermic reduction of iron oxide waste generated during the processing of ilmenite. Trans Indian Inst Met 72:11–16. https://doi.org/10.1007/s12666-018-1451-4
10. Das G-K, Pranolo Y, Zhu Z, Cheng C-Y (2013) Leaching of ilmenite ores by acidic chloride solutions. Hydrometallurgy 133:94–99. https://doi.org/10.1016/j.hydromet.2012.12.006
11. Kang J, Okabe T-H (2013) Removal of iron from titanium ore through selective chlorination using magnesium chloride. Mater Trans 54:1444–1453. https://doi.org/10.2320/matertrans.M-M2013810
12. Ward J, Bailey S, Avraamides J (1999) The use of ethylene diammonium chloride as an aeration catalyst in the removal of metallic iron from reduced ilmenite. Hydrometallurgy 53:215–232. https://doi.org/10.1016/S0304-386X(99)00046-8
13. Jha M-K, Kumar V, Singh R-J (2002) Solvent extraction of zinc from the chloride solutions. Solvent Extr Ion Exch 20:389–405. https://doi.org/10.1081/SEI-120004812
14. Niecko J (1987) Recovery of ferrous sulfate and sulfuric acid from spent pickle liquor of the steel industry. Conserv Recycl 10:309–314. https://doi.org/10.1016/0361-3658(87)90061-0
15. Lanyon M-R, Lwin T, Merritt R-R (1999) The dissolution of iron in the hydrochloric acid leach of an ilmenite concentrate. Hydrometallurgy 51:299–323. https://doi.org/10.1016/S0304-386X(98)00083-8
16. Jonglertjunya W, Rubcumintara T (2012) Titanium and iron dissolutions from ilmenite by acid leaching and microbiological oxidation techniques. Asia-Pac J Chem Eng 8:323–330. https://doi.org/10.1002/apj.1663
17. Pereira E-B, Suliman A-L, Tanabe E-H, Bertuol D-A (2018) Recovery of indium from liquid crystal displays of discarded mobile phones using solvent extraction. Miner Eng 119:67–72. https://doi.org/10.1016/j.mineng.2018.01.022
18. Hamza M-F, Roux J-C, Guibal E (2019) Metal valorization from the waste produced in the manufacturing of Co/Mo catalysts: leaching and selective precipitation. J Mater Cycles Waste Manag 21:525–538. https://doi.org/10.1007/s10163-018-0811-9
19. Busolic D, Parada F, Parra R, Sanchez M, Palacios J, Hino M (2011) Recovery of iron from copper flash smelting slags. Miner Process Extr Metall 120:32–36. https://doi.org/10.1179/037195510X12772935654945
20. Kumar V, Sahu S-K, Pandey B-D (2010) Prospects for solvent extraction processes in the Indian context for the recovery of base metals. A review. Hydrometallurgy 103:45–53. https://doi.org/10.1016/j.hydromet.2010.02.016
21. Xiang W, Liang S, Zhou Z, Qin W, Fei W (2017) Lithium recovery from salt lake brine by counter-current extraction using tributyl phosphate/$FeCl_3$ in methyl isobutyl ketone. Hydrometallurgy 171:27–32. https://doi.org/10.1016/j.hydromet.2017.04.007
22. Hu B, Nakahiro Y, Wakamatsu T (1993) The effect of organic solvents on the recovery of fine mineral particles by liquid-liquid extraction. Miner Eng 6:731–742. https://doi.org/10.1016/0892-6875(93)90004-7
23. Zhang G, Chen D, Wei G, Zhao H, Wang L, Qi T, Meng F, Meng L (2015) Extraction of iron (III) from chloride leaching liquor with high acidity using tri-n-butyl phosphate and synergistic

extraction combined with methyl isobutyl ketone. Sep Purif Technol 150:132–138. https://doi.org/10.1016/j.seppur.2015.07.001
24. Barrak H, Ahmedi R, Chevallier P, M'nif A, Laroche G, Hamzaoui A-H (2019) Highly efficient extraction of rare earth elements and others ions from green phosphoric acid medium using TMSEDTA@GO@Fe_3O_4 core-shell. Sep Purif Technol 222:145–151. https://doi.org/10.1016/j.seppur.2019.04.016
25. Amer S, Takahashi J-M, Luis A (1995) The recovery of zinc from the leach liquors of the CENIM-LNETI process by solvent extraction with di (2-ethylhexyl) phosphoric acid. Hydrometallurgy 37:323–337. https://doi.org/10.1016/0304-386X(94)00040-A
26. Tavakoli M-R, Dreisinger D-B (2013) Separation of vanadium from iron by solvent extraction using acidic and neutral organophosphorus extractants. Hydrometallurgy 141:17–23. https://doi.org/10.1016/j.hydromet.2013.10.008
27. Jackson E (1998) The solvent extraction behaviour of platinum (II) with P-50 oxime in aqueous chloride solutions. Miner Eng 11:651–656. https://doi.org/10.1016/S0892-6875(98)00049-1
28. Roosendael S-V, Roosen J, Banerjee D, Binnemans K (2019) Selective recovery of germanium from iron-rich solutions using a supported ionic liquid phase (SILP). Sep Purif Technol 221:83–92. https://doi.org/10.1016/j.seppur.2019.03.068
29. Mishra R-K, Rout P-C, Sarangi K, Nathsarma K-C (2011) Solvent extraction of Fe(III) from the chloride leach liquor of low grade iron ore tailings using Aliquat 336. Hydrometallurgy 108:93–99. https://doi.org/10.1016/j.hydromet.2011.03.003
30. Li X, Li Z, Orefice M, Binnemans K (2019) Metal recovery from spent samarium–cobalt magnets using a trichloride ionic liquid. ACS Sustain Chem Eng 7:2578–2584. https://doi.org/10.1021/acssuschemeng.8b05604
31. Ola P-D, Matsumoto M, Kondo K (2017) Recovery of Fe and Mn from aqueous solution with solvent extraction and liquid membrane permeation using ionic liquids. Desalin Water Treat 75:325–330. https://doi.org/10.5004/dwt.2017.20406
32. Song Y, Tsuchida Y, Matsumiya M, Uchino Y, Yanagi I (2018) Separation of tungsten and cobalt from WC-Co hard metal wastes using ion-exchange and solvent extraction with ionic liquid. Miner Eng 128:224–229. https://doi.org/10.1016/j.mineng.2018.08.047
33. Lu J, Dreisinger D (2014) Two-stage countercurrent solvent extraction of copper from cuprous chloride solution: Cu(II) loading coupled with Cu(I) oxidation by oxygen and iron scrubbing. Hydrometallurgy 150:41–46. https://doi.org/10.1016/j.hydromet.2014.09.003
34. Choi I, Moon G, Lee J, Jyothi R-K (2018) Hydrometallurgical processing of spent selective catalytic reduction (SCR) catalyst for recovery of tungsten. Hydrometallurgy 178:137–145. https://doi.org/10.1016/j.hydromet.2018.04.011
35. Lai W, Liu M, Li C, Suo H, Yue M (2014) Recovery of a composite powder from NdFeB slurry by co-precipitation. Hydrometallurgy 150:27–33. https://doi.org/10.1016/j.hydromet.2014.08.014
36. Mikutta C, Frommer J, Voegelin A, Kaegi R, Kretzschmar R (2010) Effect of citrate on the local Fe coordination in ferrihydrite arsenate binding, and ternary arsenate complex formation. Geochim Cosmochim Acta 74:5574–5592. https://doi.org/10.1016/j.gca.2010.06.024
37. Esalah J, Weber M-W, Vera J-H (1999) Removal of lead from aqueous solutions by precipitation with sodium di-(n-octyl) phosphinate. Sep Purif Technol 18:25–36. https://doi.org/10.1016/S1383-5866(99)00046-5
38. Esalah J, Husein M-M (2008) Removal of heavy metals from aqueous solutions by precipitation-filtration using novel organophosphorus ligands. Sep Sci Technol 43:3461–3475. https://doi.org/10.1080/01496390802219661
39. Masambi S, Dorfling C, Bradshaw S (2016) Comparing iron phosphate and hematite precipitation processes for iron removal from chloride leach solutions. Miner Eng 98:14–21. https://doi.org/10.1016/j.mineng.2016.07.001
40. Izadi A, Mohebbi A, Amiri M, Izadi N (2017) Removal of iron ions from industrial copper raffinate and electrowinning electrolyte solutions by chemical precipitation and ion exchange. Miner Eng 113:23–35. https://doi.org/10.1016/j.mineng.2017.07.018
41. Luo W, Kelly S-D, Kemner K-M, Watson D, Zhou J, Jardine P-M, Gu B (2009) Sequestering uranium and technetium through co-precipitation with aluminum in a contaminated acidic environment. Environ Sci Technol 43:7516–7522. https://doi.org/10.1021/es900731a
42. Huo L, Li W, Lu L, Cui H, Xi S, Wang J, Zhao B, Shen Y, Lu Z (2000) Preparation structure and properties of three-dimensional ordered α-Fe_2O_3 nanoparticulate film. Chem Mater 12:790–794. https://doi.org/10.1021/cm990690+
43. Brown ASC, Hargreaves JSJ, Rijniersce B (1998) A study of the structural and catalytic effects of sulfation on iron oxide catalysts prepared from goethite and ferrihydrite precursors for methane oxidation. Catal Lett 53:7–13. https://doi.org/10.1023/A:1019016830208
44. Quddus M-S, Rahman M-L, Khanam J, Biswas B, Sharmin N, Ahmed S, Tahuran NAJM (2018) Synthesis and characterization of pigment grade red iron oxide from mill scale. Int Res J Pure Appl Chem 16:1–9. https://doi.org/10.9734/IRJPAC/2018/42935
45. Muller M, Villaba J-C, Mariani F-Q, Dalpasquale M, Lemos M-Z, Huila MFG, Anaissi F-J (2015) Synthesis and characterization of iron oxide pigments through the method of the forced hydrolysis of inorganic salts. Dyes Pigm 120:271–278. https://doi.org/10.1016/j.dyepig.2015.04.026
46. Bouargane B, Marrouche A, Issiouy S-E, Biyoune M-G, Mabrouk A, Atbir A, Bachar A, Bellajrou R, Boukbir L, Bakiz B (2019) Recovery of $Ca(OH)_2$, $CaCO_3$, and Na_2SO_4 from Moroccan phosphogypsum waste. J Mater Cycles Waste Manae 21:1563–1571. https://doi.org/10.1007/s10163-019-00910-9
47. Jung C-H, Osako M (2009) Water extraction with CO_2 bubbling as pretreatment of melting-furnace fly ash for metal recovery. J Mater Cycles Waste Manag 11:65–72. https://doi.org/10.1007/s10163-008-0220-6